

Photochemically Powered AgCl Janus Micromotors as A Model System to Understand Ionic Self-diffusiophoresis

Chao Zhou, Hepeng Zhang, Jinyao Tang, and Wei Wang

Langmuir, **Just Accepted Manuscript** • DOI: 10.1021/acs.langmuir.7b04301 • Publication Date (Web): 13 Feb 2018

Downloaded from <http://pubs.acs.org> on February 17, 2018

Just Accepted

“Just Accepted” manuscripts have been peer-reviewed and accepted for publication. They are posted online prior to technical editing, formatting for publication and author proofing. The American Chemical Society provides “Just Accepted” as a service to the research community to expedite the dissemination of scientific material as soon as possible after acceptance. “Just Accepted” manuscripts appear in full in PDF format accompanied by an HTML abstract. “Just Accepted” manuscripts have been fully peer reviewed, but should not be considered the official version of record. They are citable by the Digital Object Identifier (DOI®). “Just Accepted” is an optional service offered to authors. Therefore, the “Just Accepted” Web site may not include all articles that will be published in the journal. After a manuscript is technically edited and formatted, it will be removed from the “Just Accepted” Web site and published as an ASAP article. Note that technical editing may introduce minor changes to the manuscript text and/or graphics which could affect content, and all legal disclaimers and ethical guidelines that apply to the journal pertain. ACS cannot be held responsible for errors or consequences arising from the use of information contained in these “Just Accepted” manuscripts.



Photochemically Powered AgCl Janus Micromotors as A Model System to Understand Ionic Self- diffusiophoresis

Chao Zhou,[†] H. P. Zhang,^{‡, §} Jinyao Tang,^{||} and Wei Wang^{*†}

[†] School of Materials Science and Engineering, Harbin Institute of Technology (Shenzhen),
Shenzhen 518055, China

[‡] School of Physics and Astronomy and Institute of Natural Sciences, Shanghai Jiao Tong
University, Shanghai 200240, China

[§] Collaborative Innovation Center of Advanced Microstructures, Nanjing 210093, China

^{||} Department of Chemistry, University of Hong Kong, Hong Kong SAR, 999077, China

KEYWORDS: micromotors, janus, diffusiophoresis, ultrasonic manipulation, active matter

ABSTRACT: Micromotors are an emerging class of micromachines that could find potential applications in biomedicine, environmental remediation and microscale self-assembly. Understanding their propulsion mechanisms holds the key to their future development. This is especially true for a popular category of micromotors that are driven by asymmetric surface photochemical reactions. Many of these micromotors release ionic species, and are propelled *via*

1
2
3 a mechanism termed ionic self-diffusiophoresis. But exactly how it operates remains vague. To
4
5 address this fundamental yet important issue, we have developed a dielectric-AgCl Janus
6
7 micromotor that clearly moves away from the AgCl side when exposed to UV or strong visible
8
9 light. Taking advantage of numerical simulations and acoustic levitation techniques, we have
10
11 provided tentative explanations for its speed decay over time as well as its directionality. In
12
13 addition, photoactive AgCl micromotors demonstrate interesting gravitactic behaviors that hint at
14
15 3D transport or sensing applications. The current work presents a well-controlled and easily
16
17 fabricated model system to understand chemically powered micromotors, highlighting the
18
19 usefulness of acoustic levitation for studying active matter free from the effect of boundaries.
20
21
22
23
24

25 **Introduction**

26
27
28 Understanding and exploiting powered motion at small scales sits at the core of a number of
29
30 fundamental and applied research areas, such as active matter,¹ micromachines,^{2,3}
31
32 microbiology,^{4,5} and nanomedicine.⁶⁻⁹ Although the dynamics of microorganisms (such as cells
33
34 and bacteria) and protein motors (such as kinesins and myosins) are largely understood, progress
35
36 in mimicking such biological motion with synthetic microswimmers has been small, until the
37
38 introduction of catalytic bimetallic micromotors about 15 years ago.^{10,11} Since then, a myriad of
39
40 micromotors have been developed with various mechanisms and versatile functionalities (see, for
41
42 example, ref. 7, 12-16 and references therein).
43
44
45
46
47

48 Among them, chemical reactions remain a popular choice for powering micromotors,¹⁷⁻¹⁹ and
49
50 many rely heavily on local chemical gradients.¹³ Colloids are long known to move in externally
51
52 applied chemical gradients, a mechanism termed diffusiophoresis,^{20,21} but autonomously moving
53
54 micromotors are unique for they generate their own chemical gradients locally. This is
55
56
57
58
59
60

1
2
3 conveniently termed self-diffusiophoresis,²² and is often induced by an asymmetric surface
4 reaction that consumes and releases chemical species. This reaction can be spontaneous, such as
5 the dissolution of a weakly soluble salt in water,^{23,24} and the enzymatic conversion of a substrate
6 molecule;²⁵⁻²⁸ or it can be initiated *via* external stimuli, light being a prominent example.^{29, 30}
7
8
9
10
11
12

13 Given that light can be remotely applied and easily tuned in both wavelength and intensity, light
14 powered micromotors are quickly gaining popularity.^{14,31} Many of these micromotors involve a
15 photochemical reaction that generates a local chemical gradient, and therefore moves by self-
16 diffusiophoresis. A quick survey in literature present a few notable examples based on Janus
17 structures, with parts of the particle photochemically active. These include SiO₂-Ag,³² TiO₂-SiO₂
18 ²⁹ and silver-dynabead Janus spheres,³³ and AgCl-AFP dimers,³⁴ all of which move
19 unidirectionally when exposed to ultraviolet (UV) light. The other important and common
20 feature of these systems is that they all produce ionic species, which give rise to ionic self-
21 diffusiophoresis that is responsible for the operation of a large portion of existing micromotors.
22
23 Yet, its operation mechanism still remains to be clarified. Unfortunately, existing literature can
24 only provide limited insight on this issue due to practical complications including complex
25 particle shapes, poor visual contrast to distinguish motor directionality, slow propulsion speed,
26 and the existence of multiple possible driving mechanisms, to name a few (see SI for an
27 expanded discussion). An elucidation of ionic self-diffusiophoresis is often further hindered by
28 the presence of boundaries and possible electroosmotic flows as a result.
29
30
31
32
33
34
35
36
37
38
39
40
41
42
43
44
45
46
47
48

49 As an effort to build a simple yet reliable model system to understand ionic self-diffusiophoresis,
50 we here report a AgCl Janus micromotor powered by photochemical reactions, drawing
51 inspirations from an earlier study.³⁴ When irradiated with light, this Janus particle moves away
52 from the reacting (AgCl) side and shows negative gravitaxis. Finite element simulation suggests
53
54
55
56
57
58
59
60

1
2
3 that the near-field electric field pointing from the inert to the reacting side could be the main
4
5 phoretic force that propels this Janus particle to move away from AgCl side. Our finding
6
7 introduces a photochemical micromotor with well controlled kinetics and interesting gravitactic
8
9 behaviors, and presents a renewed and microscopic view of ionic self-diffusiophoresis that
10
11 applies to a wide variety of micromotors.
12
13
14

15 **Experimental Section**

16 **Sample Synthesis and Fabrication**

17
18
19 The monolayer of PMMA microspheres was obtained following ref. 35. A concentrated
20
21 suspension of PMMA particles in ethanol was added to the surface of a thin layer of hexane
22
23 floating on water. Particles spontaneously formed a monolayer. The liquid was later pipetted out,
24
25 and the monolayer was transferred to a flat substrate (*e.g* silicon wafer). A thin layer (50 nm) of
26
27 silver was then thermally evaporated by electron beam in vacuum onto this monolayer of beads
28
29 (e-beam evaporator HHV TF500). Silver was converted into silver chloride by immersing the
30
31 silicon wafer carrying the microsphere monolayer into FeCl₃ solutions (0.01 mol/L, room
32
33 temperature for 20 min). A small amount of polyvinylpyrrolidone (PVP, 0.025 mol/L monomer
34
35 concentration) was also added into the solution to produce fine crystals of AgCl. The AgCl
36
37 morphology with and without addition of PVP is shown in Fig. S1 in the Supporting
38
39 Information. Although different in morphology, their behaviors under UV light were
40
41 qualitatively the same. Crystalline information and chemical composition of the synthesized
42
43 PMMA-AgCl Janus particles can be found in Fig. S2.
44
45
46
47
48
49
50
51

52 **Motor Experiment**

1
2
3 In a typical experiment, the Janus particles were suspended in deionized water. The
4 suspension was transferred into a rectangular capillary tube (Vitrocom, model 3520, thickness
5 200 μm), and observed under either an upright optical microscope (Olympus BX 51M) or an
6 inverted optical microscope (Olympus IX 73). Due to gravity, particles mostly sediment to the
7 bottom of the experiment cell (the capillary tube), and videos were usually recorded at this plane.
8 However, when irradiated with light, particles could float upward and eventually became trapped
9 at the “ceiling” of the capillary tube (negative gravitaxis, discussed below). The optical
10 microscope was equipped with a dual-housing adapter (model U-DULHA, Olympus) so that
11 both the halogen lamp and mercury lamp could be turned on, or be switched from one to the
12 other when needed. Videos were taken by a Point Grey camera mounted on the microscope
13 (model FL3-U3-13E4C-C) at a frame rate of 30 frames per second, and either a 20X or 50X
14 objective lens were used. Videos were then processed and analyzed by MATLAB. Particle
15 coordinates were obtained, and their trajectories and speeds can therefore be calculated.
16
17
18
19
20
21
22
23
24
25
26
27
28
29
30
31
32
33

34 **Ultrasound Experiments**

35
36
37 The ultrasonic manipulation device was fabricated based on previous reports.^{12,36} The setup was
38 constructed by attaching a piece of PZT ceramic disk (Steminc, part No. SMD12T06R412WL,
39 resonance frequency 3.4 MHz) to the back of a silicon wafer with epoxy resin. On its front side,
40 the experimental chamber (usually a rectangular capillary tube from Vitrocom) is fixed by
41 ultrasound gels directly above the ceramic disk. During the experiment, a function generator
42 (Agilent 33210A) sends a sinusoidal signal to the piezoelectric disk, which produces ultrasound
43 that propagates through the aqueous microparticle suspension in the acoustic cell. At the
44 resonance frequency, typically 3-4 MHz for our setup, particles floated up to the levitation plane
45 at the center of the acoustic cell and moved on this plane. The acoustic forces exerted on the
46
47
48
49
50
51
52
53
54
55
56
57
58
59
60

1
2
3 particle is very sensitive to the driving frequency and voltage, and one can tune it carefully so
4
5 that particles are levitated yet their light-powered autonomous motion is minimally affected by
6
7 acoustic forces. Therefore, unlike metallic microrods that show fast autonomous motion along
8
9 their long axis in the same ultrasound setup,³⁶ PMMA-AgCl Janus particles are not actively
10
11 propelled by ultrasound used in our experiment.
12
13

14 15 Numerical Simulations

16
17
18 To understand how the surface photochemical reaction provides propulsion to a PMMA-AgCl
19
20 particle, we have used a model originally developed by Velegol *et al.* for the study of self-
21
22 electrophoretic micropumps,³⁷ but more recently adapted by Velegol *et al.* and Zhang *et al.* for
23
24 the study of self-electrophoretic swimmers near a wall.^{38,39} Unlike the Janus particle in the
25
26 previous models which releases and consumes ionic fluxes at each of the hemisphere,
27
28 respectively, the Janus particle in our model produces H⁺ and Cl⁻ ions at a flux of J only at its
29
30 AgCl hemisphere, while the PMMA sphere is chemically inert. The electrical double layer
31
32 (EDL) of the particle is assumed to be infinitely thin and not significantly perturbed by the
33
34 surface reactions. The electrical boundary condition at the double layer of the AgCl hemisphere
35
36 is set by the normal potential gradients $-(\partial\phi/\partial n) = Jk_B T/2en_0(1/D^+ - 1/D^-)$, where ϕ is the electrical
37
38 potential, k_B is the Boltzmann constant, T is the temperature, e is the proton charge, n_0 is the bulk
39
40 concentration of ions, and D^+ and D^- are the diffusion coefficient of H⁺ and Cl⁻, respectively. The
41
42 electrical boundary condition at the double layer of PMMA hemisphere is $-(\partial\phi/\partial n) = 0$. Outside
43
44 EDL it is electrically neutral, and the electrostatic problem is solved by Laplace equation ($\nabla^2\phi =$
45
46 0). Fluid flows outside EDL is governed by the Stokes flow: $\eta\nabla^2\mathbf{u} = 0$, and $\nabla \cdot \mathbf{u} = 0$, where η is
47
48 the dynamic viscosity of the solution and \mathbf{u} is the fluid speed. On the surface of the PMMA-
49
50
51
52
53
54
55
56
57
58
59
60

1
2
3 AgCl, however, the flow boundary condition is governed by an electroosmotic slip velocity U_{eo}
4
5 $= \zeta \varepsilon E' / \eta$, where ε is the medium permittivity and E' is the tangential component of the local
6
7 electric field. The two hemispheres carry zeta potential of ζ_{AgCl} and ζ_{PMMA} , respectively. Finally,
8
9 the speed of the Janus particle can be calculated in one of three ways, the details of which can be
10
11 found in the Supporting Information.
12
13
14
15

16 This model was solved by a finite element package (COMSOL Multiphysics 5.2a) in a 2D
17
18 axisymmetric configuration. In the simulation model, a sphere of 2.5 μm in diameter is placed at
19
20 the center of a cylinder of 100 μm in length and 100 μm in diameter. An estimated ionic flux J of
21
22 1.6×10^{-5} mol/($\text{m}^2 \text{ s}$) was used. Details of model implementation, parameter selections and
23
24 estimations, and meshing conditions are given in the Supporting Information.
25
26
27
28
29
30

31 **Results and discussion**

32
33
34 The fabrication of the Janus microparticles is illustrated in Fig. 1a. Briefly, poly(methyl
35
36 methacrylate) (PMMA) microspheres of 2.5 μm in diameter were coated by a 50 nm layer of
37
38 silver, which was then converted to silver chloride (AgCl) by iron (III) chloride (FeCl_3)
39
40 solution.⁴⁰ The as-synthesized Janus particle had a zeta potential of -35.1 ± 3.1 mV. Details of
41
42 fabrication and characterization can be found in the Experimental Section and the Supporting
43
44 Information.
45
46
47
48
49
50
51
52
53
54
55
56
57
58
59
60

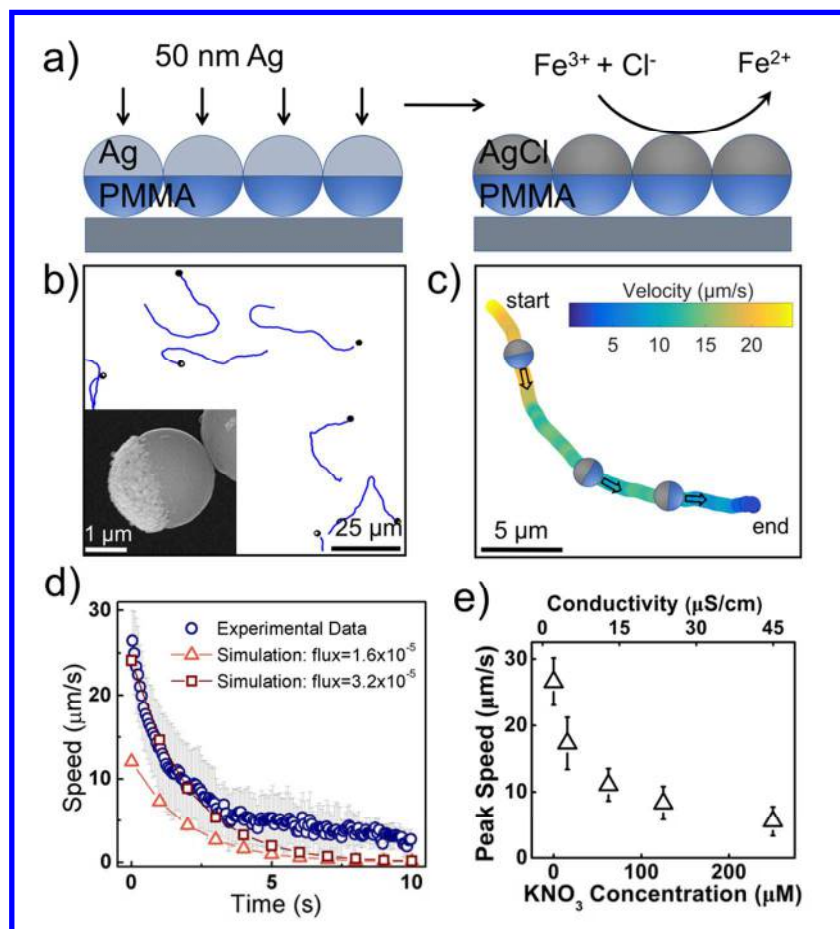
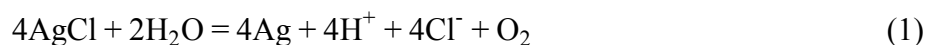


Figure 1. Dynamics of PMMA-AgCl micromotors under light. (a) The fabrication scheme of PMMA-AgCl Janus particles. (b) Particle trajectories in 7.3 s under light. Inset: a scanning electron micrograph of a PMMA-AgCl Janus particle. (c) A representative trajectory of a PMMA-AgCl micromotor of decreasing speeds (color coded) over 6.9 s. (d) Experimental speed decay profile of a Janus micromotor in 10 s (circles), with speeds simulated at surface flux of 1.6×10^{-5} (triangles) and 3.2×10^{-5} mol/(m² s) (squares). (e) Motor peak speeds as a function of solution conductivity.

When irradiated with ultraviolet (UV) light (~ 1.4 W/cm²), these PMMA-AgCl particles moved in water at considerable speeds away from the AgCl side; at long time intervals their trajectories became Brownian (Fig. 1b and Video S1). Interestingly, unlike many reported micromotors that

1
2
3 more or less maintain a constant speed over time, PMMA-AgCl micromotors slowed down
4
5 within ~10 s in a gradual and regular way until Brownian motion took over (Fig. 1c, d, Video
6
7 S2). Although speed decrease is often considered a disadvantage for micromotor applications,
8
9 why and how the micromotor slows down can provide us with valuable information on its
10
11 propulsion mechanisms (discussed later). Janus particles fabricated from polystyrene or silica
12
13 microspheres (as opposed to PMMA) were also found to consistently move away from the AgCl
14
15 side. Furthermore, PMMA-AgCl particles could also be activated by visible light ($\sim 0.1 \text{ W/cm}^2$)
16
17 of wavelengths smaller than $\sim 600 \text{ nm}$. A detailed description of particle dynamics at different
18
19 lighting conditions is given in the Supporting Information (also Video S3).
20
21
22
23

24
25 To understand the dynamics of PMMA-AgCl micromotors, we first examine the chemical
26
27 reaction occurring on their surfaces. When exposed to light of enough energy, AgCl decomposes
28
29 into Ag, following^{34,41}
30
31



33
34
35 The conversion from AgCl into Ag on the particle surface is supported by crystalline and
36
37 elemental composition characterization (Fig. S2). Note that unlike a typical heterogeneous
38
39 reaction where the concentration of a solid reactant is considered infinite, here n_{AgCl} is finite and
40
41 decreasing over time because the produced Ag coats back onto the particle and blocks further
42
43 AgCl from reacting. The apparent reaction rate v ($\text{mol}/(\text{m}^2 \text{ s})$) of this photodecomposition
44
45 averaged over the entire coated surface is therefore reasonably assumed to be linearly
46
47 proportional to the amount of AgCl left on the bead (n_{AgCl} , in mol/m^2), and we obtain:
48
49
50
51

$$52 \quad v = -\frac{dn_{\text{AgCl}}}{dt} = kn_{\text{AgCl}} = \frac{d[\text{H}^+]}{dt} = \frac{d[\text{Cl}^-]}{dt} = J \quad (2)$$

1
2
3 where J is the ionic flux (same for H^+ and Cl^- , in $mol/(m^2 s)$), k is the reaction rate constant (s^{-1})
4
5 and t is time (s). This leads to a first order reaction kinetics,
6
7

$$J = J_0 e^{-kt} \quad (3)$$

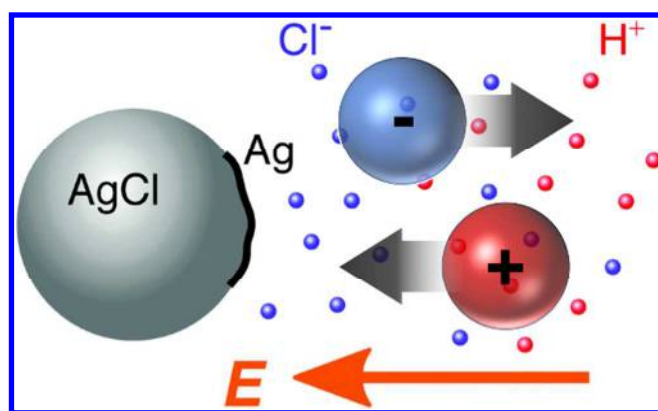
8
9
10
11 Theories³⁹ and our own simulation (introduced later) both suggest that the particle speed U
12
13 scales linearly with J . We then obtain:
14
15

$$U = U_0 e^{-kt} \quad (4)$$

16
17
18
19
20 where U_0 is the peak speed from which the motor decays over time. The particle speed profile
21
22 over time in Fig. 2d can be fit reasonably well by Eqn. 4 (fit not shown), consistent with first
23
24 order kinetics. It is worth pointing out that the speeds of these Janus motors did not reach zero in
25
26 the end, not because they were continuously but slowly propelled, but rather because our
27
28 tracking algorithm calculated an instantaneous speed of $\sim 3 \mu m/s$ for Brownian motion. This, along
29
30 with the observation that the speed decay profiles beyond ~ 5 s fit less well with exponential
31
32 decays, is discussed in more details in the Supporting Information.
33
34
35
36

37
38 The effect of solution conductivity (σ , tuned by adding different amounts of KNO_3 into the
39
40 solution) is presented in Fig 1e (see Fig. S3 for the full velocity data). Notably, micromotor peak
41
42 speeds decreased significantly at high σ , qualitatively consistent with theories for an
43
44 electrokinetic micromotor.⁴²⁻⁴⁵ We also note that the photodecomposition of $AgCl$ is a
45
46 complicated multistep process involving hypochlorous acid ($HClO$) as an important
47
48 intermediate, whose decomposition into O_2 is catalyzed by Ag^+ .⁴¹ However, adding a small
49
50 amount ($200 \mu M$) of $AgNO_3$ in the solution did not significantly change the particle dynamics
51
52 beyond the conductivity effect. Eqn.1 is therefore considered appropriate for our discussion.
53
54
55
56
57
58
59
60

1
2
3 We now focus on the origin of the particle's propulsion, and particularly why it moved away
4 from the AgCl coated side. As mentioned earlier, the local and self-generated chemical gradients
5 from the AgCl coated side. As mentioned earlier, the local and self-generated chemical gradients
6 of the ionic species in Eqn. 1 induce ionic self-diffusiophoresis (iSD). This mechanism is
7 illustrated in Fig 2 (adapted from ref. 46),⁴⁶ where a silver chloride (AgCl) microparticle
8 decomposes into silver (Ag) when illuminated and releases protons (H^+) and chloride ions (Cl^-).
9
10 Since H^+ diffuses much faster than Cl^- (diffusion coefficient 9.31×10^{-9} and 2.03×10^{-9} m^2/s ,
11 respectively), an inward electric field spontaneously forms to maintain charge neutrality in the
12 bulk. Previously, this physical picture has been used to understand how nearby positively
13 (negatively) charged microparticles were attracted towards (repelled from) the ion-releasing
14 particle, and how fascinating collective behaviors (such as schooling) emerged when every
15 particle was active.³⁴



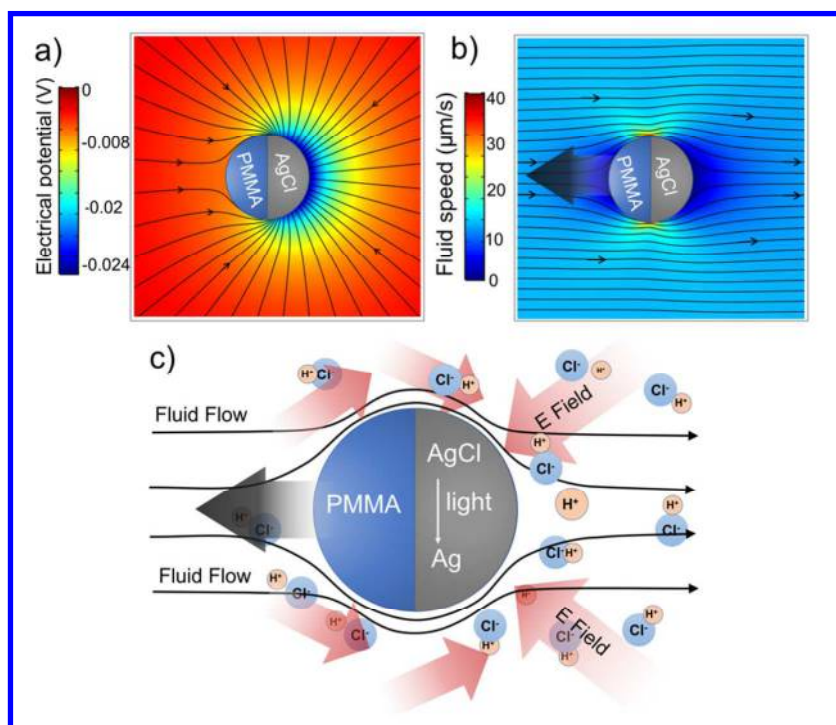
29
30
31
32
33
34
35
36
37
38
39
40
41
42
43
44
45
46
47 **Figure 2.** A typical picture of ionic diffusiophoresis near a photoactive AgCl microparticle. The
48 produced H^+ diffuse faster than Cl^- , leading to an inward electric field that moves nearby charged
49 colloidal particles (large colored spheres). Adapted and modified from Fig. 3 in ref 46 with
50 permission from the Royal Chemical Society, 2017.
51
52
53
54
55
56
57
58
59
60

1
2
3 But how does the ion-releasing particle itself move? Fig. 2 becomes less helpful in this regard
4
5 because that, although it excels in explaining the pairwise interactions and collective behaviors
6
7 among diffusiophoretic particles,^{29,32,34,47-49} it looks at the electric field around the particle with a
8
9 far field approximation. If we, for example, consider the electric field depicted in Fig. 2 that is
10
11 pointing to the left, electrophoretic motion of a negatively charged PMMA-AgCl particle
12
13 towards the AgCl side entails, whereas in our experiments they move in the opposite direction.
14
15 As we have noted earlier, there is no satisfactory explanation/prediction in the literature on how
16
17 the ion-releasing Janus particle moves due to various complications.
18
19
20

21
22 The solution to this inconsistency could lie in the distribution of electric and flow fields around
23
24 the entirety of a moving Janus particle, including the near-field components, solved by finite
25
26 element simulations (COMSOL Multiphysics, see SI for details). Specifically, the results in Fig.
27
28 3a show a lower electrical potential near the AgCl cap and an electric field that consequently
29
30 points inward in the far field, both in agreement with Fig. 2. However, the simulation also
31
32 reveals additional electric field lines that point from the PMMA towards the AgCl hemisphere in
33
34 the near field that, when coupled with the negative surface charges, create a slip velocity
35
36 pointing in the same direction (Fig. 3b). It is *this* slip flow, we argue, that causes the motor to
37
38 move away from the AgCl side. Our refreshed operating mechanism of ionic self-
39
40 diffusiophoresis is summarized in Fig. 3c.
41
42
43
44
45

46
47 Not only is our model capable of explaining the directionality of Janus motors, it also solves for
48
49 the motor speeds using the experimentally measured reaction rate constant k (see SI for details).
50
51 Two major assumptions were made: 1) only a thin layer of AgCl participated in the reaction; 2) k
52
53 (the reaction rate constant, acquired by fitting the speed profile for the first 3 s) remained
54
55 unchanged during the reaction. An initial ion flux J of $\sim 1.6 \times 10^{-5}$ mol/(m² s) was then estimated,
56
57
58
59
60

1
2
3 leading to particle speeds that decay exponentially from a peak speed of $\sim 12 \mu\text{m/s}$, which is
4
5 roughly half of the experimental value shown in Fig. 1d. Our simulation also suggests the
6
7 particle speed scales to $J(D_{\text{H}^+}-D_{\text{Cl}^-})$ (Fig. S12, S14), consistent with theories.⁴³ We acknowledge
8
9 that the current numerical model is far from perfect, and serves better as a qualitative guide than
10
11 a quantitative prediction. Inaccuracies could stem from the much-simplified estimation of the
12
13 amount of reactive AgCl, or the fact that surface charges are prone to change as a result of
14
15 surface reactions. Further improvements are under way.
16
17
18
19



20
21
22
23
24
25
26
27
28
29
30
31
32
33
34
35
36
37
38
39
40
41
42
43
44
45
46
47
48
49
50
51
52
53
54
55
56
57
58
59
60

Figure 3. Finite element simulation of PMMA-AgCl micromotors. (a) Electrical potential (V , color coded) and electric field (black arrows) distribution around a Janus particle. (b) Fluid speed magnitude (color coded) and flow field lines (black arrows) in the reference frame of a Janus particle, which moves away from the AgCl side in the lab frame. (c) Schematics of how a PMMA-AgCl micromotor moves.

1
2
3 To corroborate our proposed mechanism of ionic self-diffusiophoresis, we consider two
4
5 complicating factors starting with possible mechanisms other than ionic self-diffusiophoresis that
6
7 could contribute to the motion of PMMA-AgCl particles. For example, the produced O₂ (or
8
9 HClO) in Eqn. 1, one might argue, suggests the possibility of bubble propulsion or non-ionic
10
11 diffusiophoresis. Bubble propulsion, a mechanism responsible for a major category of
12
13 micromotors that jet through water by bubble recoil,^{50, 51} can be readily eliminated since no
14
15 bubble was observed in the vicinity of moving Janus particles. Non-ionic diffusiophoresis, on the
16
17 other hand, is a controversial issue,^{43,44,52} and there is, to the best of our knowledge, no
18
19 indisputable proof that the production of dissolved O₂ or HClO alone can propel micromotors at
20
21 ~10 μm/s at the flux magnitude in our experiment. In addition, the observed scaling law between
22
23 particle speed and solution conductivity in Fig. 2e strongly suggests an electrokinetic effect. The
24
25 contribution of non-ionic products is therefore believed to be small.
26
27
28
29

30
31 One might also wonder if thermal effects contribute in the form of thermophoresis. This could be
32
33 due to, for example, the photodecomposition of AgCl. However, numerical simulation shows a
34
35 negligible temperature gradient across the particle from the reaction enthalpy change
36
37 (endothermic, $\Delta H_f = 102.79$ kJ/mol) and reaction rates. Moreover, since AgCl is known to
38
39 decompose in light, we do not expect it to show a strong photothermal effect. Ag nanoparticles,
40
41 on the other hand, are known to show strong plasmonic resonance in the visible spectrum.
42
43 However, thermophoresis due to photothermal Ag nanoparticles would lead to faster motors as
44
45 the conversion from AgCl to Ag progressed, while the opposite speed profile was observed. We
46
47 further confirm that neither PMMA-Ag Janus particles before conversion to AgCl, nor PMMA-
48
49 AgCl Janus particles after long time light exposure, showed any directional motion beyond
50
51 Brownian motion when irradiated with light (see Fig. S7), strongly suggesting that the particle's
52
53
54
55
56
57
58
59
60

1
2
3 motion was associated with the decomposition of AgCl instead of thermal effects of Ag. The
4 possible contributions from heat, bubbles or non-ionic diffusiophoresis are therefore regarded as
5 negligible as compared to the ionic diffusiophoresis mechanism we proposed.
6
7
8
9

10
11 Finally, we consider the bottom substrates that Janus particles reside on (or not, see below), and
12 how it may or may not affect the particle dynamics. The boundary issue arises in light of recent
13 studies that have shown how charged boundaries can significantly affect the speed and
14 directionality of nearby phoretic micromotors *via* hydrodynamic, electrostatic or phoretic
15 effects.^{38,39,53-55} One might then argue that this boundary effect also applies to PMMA-AgCl
16 particles, which naturally sediment, and changes their speeds or directionality. The most
17 straightforward response to this argument is to examine the particle dynamics in the bulk
18 solution far away from any boundary, but this has been experimentally challenging due to the
19 fact that Janus particles are often heavier than water and naturally sediment.
20
21
22
23
24
25
26
27
28
29
30
31

32
33 To address this issue, we designed an ultrasonically manipulation device to trap particles on a
34 pressure nodal plane by megahertz acoustic standing waves (Fig. 4a),^{12,36} the principle of which
35 has been widely studied and exploited in the field of microfluidics and acoustofluidic devices.⁵⁶⁻
36
37
38
39
40 ⁵⁸ On this levitation plane ~ 100 μm away from either the top or bottom surface (Video S4),
41 illuminated PMMA-AgCl particles moved away from the AgCl side with speed profiles
42 comparable to when they were near boundaries. These results strongly suggest that boundaries
43 had minor effect on either the speed or the directionality of AgCl Janus micromotors. Since the
44 focus of the current study is on the individual dynamics of AgCl micromotors, we leave the
45 discussion on this interesting and somewhat surprising insensitivity to walls to a future study.
46
47
48
49
50
51
52
53
54
55
56
57
58
59
60

1
2
3 An interesting consequence of the PMMA-AgCl micromotors moving away from the AgCl side
4 is its negative gravitaxis (Fig. 4b, Video S5, S6): some particles that were initially settled at the
5 cell bottom could, when irradiated with strong light, rise up in the z direction and out of focus. In
6
7
8
9
10 ~10 s they reached the top cell cover (cell height ~200 μm), where they resumed 2D activity and
11
12 gradually slowed down. A quantitative comparison between their dynamics at the bottom, in the
13
14 bulk, and at the surface, however, is challenging due to limitations of tracking techniques as well
15
16 as their gradual loss in speeds. We also note that these gravitactic particles were not permanently
17
18 trapped at the top boundary; they readily sediment if light was turned off, or if their speeds
19
20 decayed below a certain level (threshold not measured). Such negative gravitaxis might be
21
22 explained by a simple density argument: since AgCl has a higher density (5.56 g/cm^3) than water
23
24 and PMMA (1.18 g/cm^3), the AgCl side of the Janus particle preferably orients towards the
25
26 bottom and, when activated by light, propels the particle upward and away from the AgCl side.
27
28
29
30 Such a preferred orientation was experimentally confirmed for PMMA-AgCl particles
31
32 sedimented near a substrate under weak light, which shows a probability of 64.5% having the
33
34 AgCl cap tilted downward (statistics acquired from 45 Janus spheres, see SI and Fig. S8 for
35
36
37
38 details).
39
40
41
42
43
44
45
46
47
48
49
50
51
52
53
54
55
56
57
58
59
60

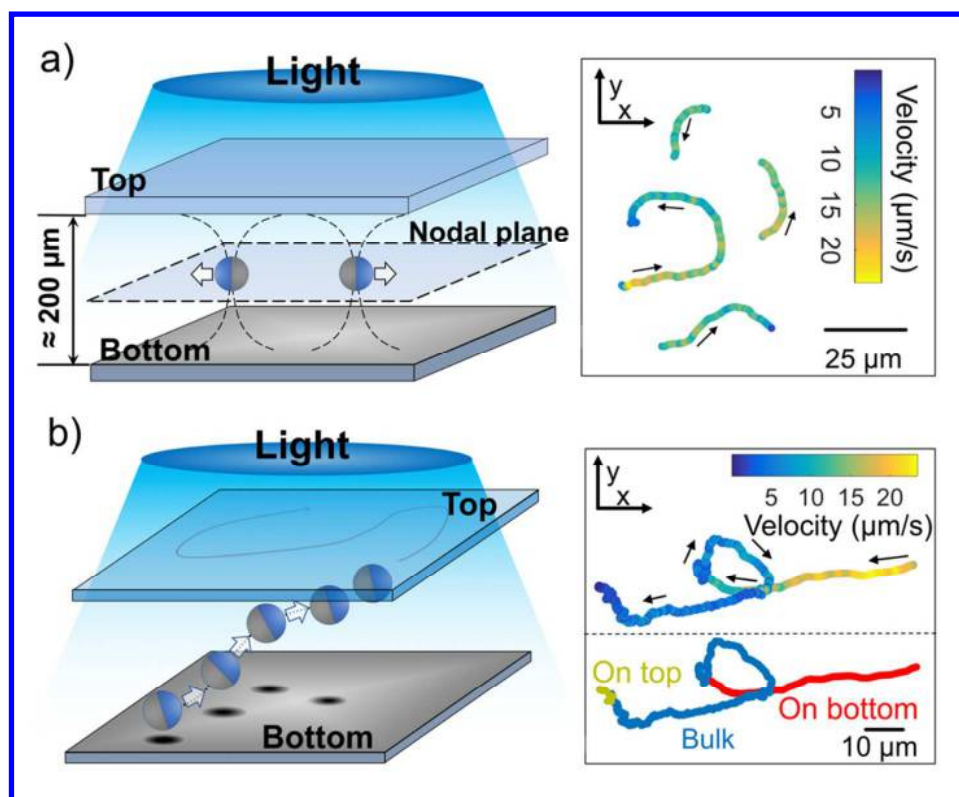


Figure 4. The effect of boundaries on light driven PMMA-AgCl micromotors. (a) Motors are levitated by acoustic standing waves and move in the bulk solution away from the AgCl side (silver color) after the ultrasound was turned off. A few representative trajectories are presented on the right, with particle velocities color coded. (b) Motors undergo gravitaxis under light and move from the bottom to the top of the experimental cell. One representative motor trajectory from the bottom to the top of the cell is presented on the right.

Gravitactic micromotors were previously observed for chemically propelled Janus micromotors,^{59,60} but light-induced negative gravitaxis opens up new and interesting possibilities. For example, one can imagine that these gravitactic micromotors act like scuba divers and can, when cued by light, transport cargos or analytes located at the bottom or in the bulk solution to

1
2
3 the surface, where further analysis or assembly awaits. When the mission is finished or their
4 service is no longer needed, particles dive back down, waiting to be summoned again. This kind
5 of activated but independent “commute” between the bulk and an interface is significantly
6 different from almost any kind of micromotors to date that only dwell near an interface, and
7 enables the autonomous yet controlled exploration of their 3D environments. Although this
8 vision is tempting, we acknowledge the limitation of the current AgCl micromotors such as their
9 short lifetimes and long response times, both on the order of seconds. In addition, AgCl
10 micromotors consumes their active chemicals (AgCl) over time and are therefore not reusable or
11 sustainable, although efforts on recycled micromotors based on silver halide have been
12 reported.⁶¹ Improvement of the photoactivated Janus micromotor and a more thorough study of
13 its gravitactic effect is currently underway.

29 **Conclusion**

30
31
32 To summarize, we have developed a photoactive dielectric-AgCl Janus motors that, when
33 illuminated with UV or strong visible light, moved away from the AgCl side and showed
34 negative gravitaxis. The photodecomposition of AgCl into H^+ and Cl^- are believed to induce
35 ionic self-diffusiophoresis, leading to an exponential speed decay. Through control experiments
36 far from any boundaries, combined with finite element simulation, the moving direction of
37 PMMA-AgCl micromotors is believed to be due to the near-field slip flow from the uncoated to
38 the coated side. These motors also showed negative gravitaxis and creamed to the top surface
39 when illuminated, a potentially useful feature for sensing applications and cargo transport in 3D.
40 The current study improves our understanding of ionic self-diffusiophoresis, and might shed
41 light on the future designs of chemically powered micro- and nanomachines. Additionally, the
42
43
44
45
46
47
48
49
50
51
52
53
54
55
56
57
58
59
60

1
2
3 unique benefit of acoustic levitation demonstrated in this study opens up great opportunities for
4
5 studying active matter away from boundaries.
6
7
8
9
10

11 ASSOCIATED CONTENT

12 13 14 15 **Supporting Information.**

16
17
18 The Supporting Information is available free of charge on the ACS Publications website at DOI:
19
20 xxx.
21
22

23 A literature survey of reports on ionic self-diffusiophoresis, figures of sample synthesis and
24
25 particle dynamics at different experimental conditions, a brief discussion on the effect of
26
27 different lighting conditions, numerical simulation details, and description of video files. (file
28
29 type, PDF)
30
31

32 Six supporting videos (file type, AVI)
33
34
35

36 AUTHOR INFORMATION

37 38 **Corresponding Author**

39
40
41 *E-mail: weiwangsz@hit.edu.cn, or wwang.hitsz@gmail.com.
42
43

44 **Funding Sources**

45
46 This project is financially supported by the National Natural Science Foundation of China
47
48 (11774075, 11402069 and 11422427), Natural Science Foundation of Guangdong Province (No.
49
50 2107B030306005), the Science Technology and Innovation Program of Shenzhen
51
52
53
54
55
56
57
58
59
60

(JCYJ20170307150031119), and the Program for Professor of Special Appointment at Shanghai Institutions of Higher Learning Grant.

ACKNOWLEDGMENT

The authors would like to thank Prof. Thomas Mallouk, Ayusman Sen, Darrell Velegol, John Gibbs and Dr. Himanagamasana Kandula for their extremely helpful discussions, and Xiaobin Fan for the help with light power density measurement.

REFERENCES

- (1) Ramaswamy, S. The Mechanics and Statistics of Active Matter. *Annu. Rev. Condens. Matter Phys.* **2010**, *1*, 323-345.
- (2) Wang, J. *Nanomachines: Fundamentals and Applications*. John Wiley & Sons: Hoboken, 2013.
- (3) Mallouk, T. E.; Sen, A. Powering Nanorobots. *Sci. Am.* **2009**, *300*, 72-77.
- (4) Lauga, E.; Powers, T. R. The Hydrodynamics of Swimming Microorganisms. *Rep. Prog. Phys.* **2009**, *72*, 096601.
- (5) Purcell, E. M. Life at Low Reynolds Number. *Am. J. Phys.* **1977**, *45*, 3-11.
- (6) Peng, F.; Tu, Y.; Wilson, D. A. Micro/Nanomotors Towards *in Vivo* Application: Cell, Tissue and Biofluid. *Chem. Soc. Rev.* **2017**, *46*, 5289-5310.
- (7) Li, J.; de Ávila, B. E.-F.; Gao, W.; Zhang, L.; Wang, J. Micro/Nanorobots for Biomedicine: Delivery, Surgery, Sensing, and Detoxification. *Sci. Rob.* **2017**, *2*, 6431.
- (8) Jain, R. K.; Stylianopoulos, T. Delivering Nanomedicine to Solid Tumors. *Nat. Rev. Clin. Oncol.* **2010**, *7*, 653-664.
- (9) Martel, S. Journey to the Center of a Tumor. *IEEE Spectrum* **2012**, *49*, 45-53.
- (10) Fournier-Bidoz, S.; Arsenault, A. C.; Manners, I.; Ozin, G. A. Synthetic Self-Propelled Nanorobots. *Chem. Commun.* **2005**, 441-443.
- (11) Paxton, W. F.; Kistler, K. C.; Olmeda, C. C.; Sen, A.; St. Angelo, S. K.; Cao, Y.; Mallouk, T. E.; Lammert, P. E.; Crespi, V. H. Catalytic Nanomotors: Autonomous Movement of Striped Nanorods. *J. Am. Chem. Soc.* **2004**, *126*, 13424-13431.
- (12) Rao, K. J.; Li, F.; Meng, L.; Zheng, H.; Cai, F.; Wang, W. A Force to Be Reckoned With: A Review of Synthetic Microswimmers Powered by Ultrasound. *Small* **2015**, *11*, 2836-2846.
- (13) Wang, W.; Duan, W.; Ahmed, S.; Mallouk, T. E.; Sen, A. Small Power: Autonomous Nano- and Micromotors Propelled by Self-Generated Gradients. *Nano Today* **2013**, *8*, 531-554.

- 1
2
3 (14) Xu, L.; Mou, F.; Gong, H.; Luo, M.; Guan, J. Light-Driven Micro/Nanomotors: From
4 Fundamentals to Applications. *Chem. Soc. Rev.* **2017**, *46*, 6905-6926.
5
6 (15) Lin, X.; Si, T.; Wu, Z.; He, Q. Self-Thermophoretic Motion of Controlled Assembled
7 Micro-/Nanomotors. *Phys. Chem. Chem. Phys.* **2017**, *19*, 23606.
8
9 (16) Xu, T.; Gao, W.; Xu, L. P.; Zhang, X.; Wang, S. Fuel-Free Synthetic Micro-/Nanomachines.
10 *Adv. Mater.* **2016**, *29*, 1603250.
11
12 (17) Colberg, P. H.; Reigh, S. Y.; Robertson, B.; Kapral, R. Chemistry in Motion: Tiny Synthetic
13 Motors. *Acc. Chem. Res.* **2014**, *47*, 3504-3511.
14
15 (18) Dey, K. K.; Sen, A. Chemically Propelled Molecules and Machines. *J. Am. Chem. Soc.*
16 **2017**, *139*, 7666-7676.
17
18 (19) Sánchez, S.; Soler, L.; Katuri, J. Chemically Powered Micro-and Nanomotors. *Angew.*
19 *Chem., Int. Ed.* **2015**, *54*, 1414-1444.
20
21 (20) Ebel, J.; Anderson, J. L.; Prieve, D. Diffusiophoresis of Latex Particles in Electrolyte
22 Gradients. *Langmuir* **1988**, *4*, 396-406.
23
24 (21) Velegol, D.; Garg, A.; Guha, R.; Kar, A.; Kumar, M. Origins of Concentration Gradients for
25 Diffusiophoresis. *Soft Matter* **2016**, *12*, 4686-4703.
26
27 (22) Popescu, M. N.; Uspal, W. E.; Dietrich, S. Self-Diffusiophoresis of Chemically Active
28 Colloids. *Eur. Phys. J-Spec. Top.* **2016**, *225*, 2189-2206.
29
30 (23) Guix, M.; Meyer, A. K.; Koch, B.; Schmidt, O. G. Carbonate-Based Janus Micromotors
31 Moving in Ultra-Light Acidic Environment Generated by Hela Cells *in Situ*. *Sci. Rep.* **2016**,
32 *6*, 1-7.
33
34 (24) McDermott, J. J.; Kar, A.; Daher, M.; Klara, S.; Wang, G.; Sen, A.; Velegol, D. Self-
35 Generated Diffusioosmotic Flows from Calcium Carbonate Micropumps. *Langmuir* **2012**,
36 *28*, 15491-15497.
37
38 (25) Gáspár, S. Enzymatically Induced Motion at Nano-and Micro-Scales. *Nanoscale* **2014**, *6*,
39 7757-7763.
40
41 (26) Ma, X.; Hortelão, A. C.; Patiño, T.; Sánchez, S. Enzyme Catalysis to Power
42 Micro/Nanomachines. *ACS Nano* **2016**, *10*, 9111-9122.
43
44 (27) Dey, K. K.; Zhao, X.; Tansi, B. M.; Méndez-Ortiz, W. J.; Córdova-Figueroa, U. M.;
45 Golestanian, R.; Sen, A. Micromotors Powered by Enzyme Catalysis. *Nano Lett.* **2015**, *15*,
46 8311-8315.
47
48 (28) Ma, X.; Jannasch, A.; Albrecht, U.-R.; Hahn, K.; Miguel-López, A.; Schäffer, E.; Sánchez,
49 S. Enzyme-Powered Hollow Mesoporous Janus Nanomotors. *Nano Lett.* **2015**, *15*, 7043-
50 7050.
51
52 (29) Hong, Y.; Diaz, M.; Córdova-Figueroa, U. M.; Sen, A. Light-Driven Titanium-Dioxide-
53 Based Reversible Microfireworks and Micromotor/Micropump Systems. *Adv. Funct. Mater.*
54 **2010**, *20*, 1568-1576.
55
56 (30) Chen, C.; Mou, F.; Xu L.; Wang, S; Guan J.; Feng, Z.; Wang, Q.; Kong, L.; Li, W. Wang, J.;
57 Zhang, Q. Semiconductors: Light-Steered Isotropic Semiconductor Micromotors. *Adv.*
58 *Mater.* **2017**, *29*, 163374.
59
60

- 1
2
3 (31) Chen, H.; Zhao, Q.; Du, X. Light-Powered Micro/Nanomotors. *Micromachines*. **2018**, *9*, 1-
4 19.
5
6 (32) Sen, A.; Ibele, M.; Hong, Y.; Velegol, D. Chemo and Phototactic Nano/Microbots. *Faraday*
7 *Discuss.* **2009**, *143*, 15-27.
8
9 (33) Chaturvedi, N.; Hong, Y.; Sen, A.; Velegol, D. Magnetic Enhancement of Phototaxing
10 Catalytic Motors. *Langmuir* **2010**, *26*, 6308-6313.
11
12 (34) Ibele, M.; Mallouk, T. E.; Sen, A. Schooling Behavior of Light-Powered Autonomous
13 Micromotors in Water. *Angew. Chem., Int. Ed.* **2009**, *48*, 3308-3312.
14
15 (35) Goldenberg, L. M.; Wagner, J.; Stumpe, J.; Paulke, B.-R.; Görnitz, E. Simple Method for
16 the Preparation of Colloidal Particle Monolayers at the Water/Alkane Interface. *Langmuir*
17 **2002**, *18*, 5627-5629.
18
19 (36) Wang, W.; Castro, L. A.; Hoyos, M.; Mallouk, T. E. Autonomous Motion of Metallic
20 Microrods Propelled by Ultrasound. *ACS Nano* **2012**, *6*, 6122-6132.
21
22 (37) Kline, T. R.; Iwata, J.; Lammert, P. E.; Mallouk, T. E.; Sen, A.; Velegol, D. Catalytically
23 Driven Colloidal Patterning and Transport. *J. Phys. Chem. B* **2006**, *110*, 24513-24521
24
25 (38) Chiang, T.-Y.; Velegol, D. Localized Electroosmosis (LEO) Induced by Spherical Colloidal
26 Motors. *Langmuir* **2014**, *30*, 2600-2607.
27
28 (39) Liu, C.; Zhou, C.; Wang, W.; Zhang, H. Bimetallic Microswimmers Speed up in Confining
29 Channels. *Phys. Rev. Lett.* **2016**, *117*, 198001.
30
31 (40) Bi, Y.; Ye, J. *In Situ* Oxidation Synthesis of Ag/AgCl Core-Shell Nanowires and Their
32 Photocatalytic Properties. *Chem. Commun.* **2009**, 6551-6553.
33
34 (41) Calzaferri, G. At the Time He Made the First Photographs on Paper: Did Henry Fox Talbot
35 Oxidize Water to Oxygen with Sunlight? *Catal. Today* **1997**, *39*, 145-157.
36
37 (42) Paxton, W. F.; Baker, P. T.; Kline, T. R.; Wang, Y.; Mallouk, T. E.; Sen, A. Catalytically
38 Induced Electrokinetics for Motors and Micropumps. *J. Am. Chem. Soc.* **2006**, *128*, 14881-
39 14888.
40
41 (43) Brown, A. T.; Poon, W. C.; Holm, C.; de Graaf, J. Ionic Screening and Dissociation Are
42 Crucial for Understanding Chemical Self-Propulsion in Polar Solvents. *Soft Matter* **2017**,
43 *13*, 1200-1222.
44
45 (44) Brown, A. T.; Poon, W. C. Ionic Effects in Self-Propelled Pt-Coated Janus Swimmers. *Soft*
46 *Matter* **2014**, *10*, 4016-4027.
47
48 (45) Moran, J. L.; Posner, J. D. Role of Solution Conductivity in Reaction Induced Charge Auto-
49 Electrophoresis. *Phys. Fluids* **2014**, *26*, 042001.
50
51 (46) Illien, P.; Golestanian, R.; Sen, A. 'Fuelled' motion: Phoretic Motility and Collective
52 Behaviour of Active Colloids. *Chem. Soc. Rev.* **2017**, *46*, 5508-5518.
53
54 (47) Ibele, M. E.; Lammert, P. E.; Crespi, V. H.; Sen, A. Emergent, Collective Oscillations of
55 Self-Mobile Particles and Patterned Surfaces under Redox Conditions. *ACS Nano* **2010**, *4*,
56 4845-4851.
57
58
59
60

- 1
2
3 (48) Duan, W.; Liu, R.; Sen, A. Transition between Collective Behaviors of Micromotors in
4 Response to Different Stimuli. *J. Am. Chem. Soc.* **2013**, *135*, 1280-1283.
5
6 (49) Altemose, A.; Sánchez-Farrán, M. A.; Duan, W.; Schulz, S.; Borhan, A.; Crespi, V. H.; Sen,
7 A. Chemically-Controlled Spatiotemporal Oscillations of Colloidal Assemblies. *Angew.*
8 *Chem., Int. Ed.* **2017**, *129*, 7925-7929.
9
10 (50) Mei, Y.; Huang, G.; Solovev, A. A.; Ureña, E. B.; Mönch, I.; Ding, F.; Reindl, T.; Fu, R. K.;
11 Chu, P. K.; Schmidt, O. G. Versatile Approach for Integrative and Functionalized Tubes by
12 Strain Engineering of Nanomembranes on Polymers. *Adv. Mater.* **2008**, *20*, 4085-4090.
13
14 (51) Magdanz, V.; Guix, M.; Schmidt, O. G. Tubular Micromotors: From Microjets to
15 Spermboats. *Rob. Biomimetics* **2014**, *1*, 11.
16
17 (52) Ebbens, S.; Gregory, D.; Dunderdale, G.; Howse, J.; Ibrahim, Y.; Liverpool, T.;
18 Golestanian, R. Electrokinetic Effects in Catalytic Platinum-Insulator Janus Swimmers.
19 *EPL* **2014**, *106*, 58003.
20
21 (53) Uspal, W.; Popescu, M. N.; Dietrich, S.; Tasinkevych, M. Self-Propulsion of a Catalytically
22 Active Particle near a Planar Wall: From Reflection to Sliding and Hovering. *Soft Matter*
23 **2015**, *11*, 434-438.
24
25 (54) Das, S.; Garg, A.; Campbell, A. I.; Howse, J.; Sen, A.; Velegol, D.; Golestanian, R.;
26 Ebbens, S. J. Boundaries Can Steer Active Janus Spheres. *Nat. Commun.* **2015**, *6*, 8999.
27
28 (55) Simmchen, J.; Katuri, J.; Uspal, W. E.; Popescu, M. N.; Tasinkevych, M.; Sánchez, S.
29 Topographical Pathways Guide Chemical Microswimmers. *Nat. Commun.* **2016**, *7*, 10598.
30
31 (56) Gröschl, M. Ultrasonic Separation of Suspended Particles-Part I: Fundamentals. *Acta Acust.*
32 *Acust.* **1998**, *84*, 432-447.
33
34 (57) Evander, M.; Nilsson, J. Acoustofluidics 20: Applications in Acoustic Trapping. *Lab Chip*
35 **2012**, *12*, 4667-4676.
36
37 (58) Shi, J.; Ahmed, D.; Mao, X.; Lin, S.-C. S.; Lawit, A.; Huang, T. J. Acoustic Tweezers:
38 Patterning Cells and Microparticles Using Standing Surface Acoustic Waves (SSAW). *Lab*
39 *Chip* **2009**, *9*, 2890-2895.
40
41 (59) Takatori, S. C.; De Dier, R.; Vermant, J.; Brady, J. F. Acoustic Trapping of Active Matter.
42 *Nat. Commun.* **2016**, *7*, 10694.
43
44 (60) Campbell, A. I.; Ebbens, S. J. Gravitaxis in Spherical Janus Swimming Devices. *Langmuir*
45 **2013**, *29*, 14066-14073.
46
47 (61) Wong, F.; Sen, A. Progress toward Light-Harvesting Self-Electrophoretic Motors: Highly
48 Efficient Bimetallic Nanomotors and Micropumps in Halogen Media. *ACS Nano* **2016**, *10*,
49 7172-7179.
50

51 For Table of Contents Use Only
52
53
54
55
56
57
58
59
60

